Inorg. Chem. **2005**, *44*, 1073–1081

Conducting Polymers Containing In-Chain Metal Centers: Electropolymerization of Oligothienyl-Substituted {M(tpy)$_2$} Complexes and in Situ Conductivity Studies, M = Os(II), Ru(II)

Johan Hjelm,[†] Robyn W. Handel,[‡] Anders Hagfeldt,[†] Edwin C. Constable,*[,‡] Catherine E. Housecroft,[‡] and Robert J. Forster*[,§]

Department of Physical Chemistry, Uppsala University, Box 579, SE-751 23, Uppsala, Sweden, National Centre for Sensor Research, Dublin City University, Glasnevin, Dublin 9, Ireland, and Department of Chemistry, University of Basel, Spitalstrasse 51, CH-4056, Switzerland

Received June 15, 2004

The electropolymerization of a series of Ru and Os bis-terpyridine complexes that form rodlike polymers with bithienyl, quaterthienyl, or hexathienyl bridges has been studied. Absorption spectroscopy, scanning electron microscopy, and cyclic voltammetry have been used to characterize the monomers and resulting polymer films. The absolute dc conductivity of the quaterthienyl-bridged {Ru(tpy)$_2$} and {Os(tpy)$_2$} polymers is unusually large and independent of the identity of the metal center at 1.6×10^{-3} S cm^{-1}. The maximum conductivity occurs at the formal potential of each redox process, which typically is observed for systems where redox conduction is the dominant charge transport mechanism. Significantly, the dc conductivity of the metal-based redox couple observed in these polymers is 2 orders of magnitude higher than that of a comparable nonconjugated system.

Introduction

Transition-metal/polythiophene hybrid materials is an interesting group of materials within the rapidly growing class that consists of conjugated polymers with transition metals linked to or directly in the π-conjugated polymer backbone.[1−3] They are of particular interest since they allow the electronic, optical, and catalytic properties of metal complexes[3] to be incorporated within a polymer film that can be deposited in precise locations.

Polymers, such as polythiophene hybrid materials in which ferrocenyl or transition-metal bis(salicylidenimine) groups have been incorporated in the backbone, are appealing for investigations of the effects of matching the redox potentials of the bridge and the metal centers on the material's conductivity.[4−6] These materials are both electronically segmented in nature, and the thiophene−bis(salicylidenimine) complex polymer showed a marked dependence of conductivity on the interchain spacing. Two limiting cases can be distinguished for DC electron conductivity in electroactive polymers: first, charge delocalization along the backbone and the migration of polarons and bipolarons, in a way that is similar to that found in organic conjugated polymers such as polythiophene; and second, charge hopping between localized redox centers within the polymer.[1,3,7] In electronically segmented polymers, such as those reported here, we expect charge transport to be governed mainly by electron hopping within and between chains.

In this paper, the electropolymerization of a series of Ru and Os bis-terpyridine complexes that form rodlike polymers with bithienyl, quaterthienyl, or hexathienyl bridges is reported. A key objective of the work is to optimize the dynamics of charge propagation by bringing the thienyl bridge and metal-center-based redox processes into resonance through tuning of the redox potentials of the bridge. Here, we report the synthesis, characterization, electropolymerization, and in situ conductivity studies of some of these polymer films.

* Authors to whom correspondence should be addressed. E-mail: robert.forster@dcu.ie (R.J.F.); Edwin.Constable@unibas.ch (E.C.C.).
[†] Uppsala University.
[‡] University of Basel.
[§] Dublin City University.

(1) Pickup, P. G. *J. Mater. Chem.* **1999**, *9*, 1641.
(2) Kingsborough, R. P.; Swager, T. M. *Prog. Inorg. Chem.* **1999**, *48*, 123.
(3) Wolf, M. O. *Adv. Mater.* **2001**, *13*, 545.
(4) Zhu, Y.; Wolf, M. O. *J. Am. Chem. Soc.* **2000**, *122*, 10121.
(5) Zhu, Y.; Wolf, M. O. *Chem. Mater.* **1999**, *11*, 2995.
(6) Kingsborough, R. P.; Swager, T. M. *J. Am. Chem. Soc.* **1999**, *121*, 8825.
(7) Lyons, M. E. G. In *Electroactive Polymer Electrochemistry, Part 1: Fundamentals*; Lyons, M. E. G., Ed.; Plenum Press: New York, 1994; p 1.

10.1021/ic049221m CCC: $30.25
Published on Web 01/26/2005

Chart 1. Structures of Ligands and Ring Labeling Used in the Experimental Section

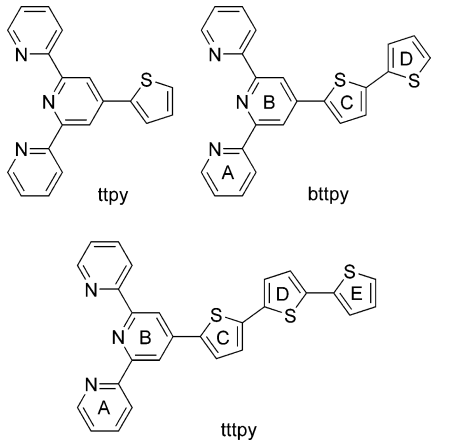

Experimental Section

Materials and Reagents. Tetra-*n*-butylammonium tetrafluoroborate, [*n*-Bu_4N][BF_4] (Aldrich), was dried for at least 12 h in a vacuum oven at 80 °C before use. BF_3·OEt_2 (Aldrich, purified, redistilled) and acetonitrile (Aldrich, anhydrous) used in the electrochemical experiments were used as received. *N*-Ethylmorpholine, [NH_4][PF_6], $K_2[OsCl_6]$, $RuCl_3$·$3H_2O$, ethane-1,2-diol, and 2-acetalpyridine were purchased from Aldrich and used as received. K[^{t}BuO] was dried in a desiccator under vacuum before use. Dry tetrahydrofuran (THF) was freshly distilled from sodium/benzophenone before use. The syntheses of the ligands ttpy (Chart 1),[8,9] bttpy,[10] and the complexes [M(ttpy)$_2$][PF_6]$_2$ (M = Ru, Os)[8,9] and [Os(bttpy)$_2$][PF_6]$_2$[10] have been previously published.

Procedures and Instrumentation. ^{1}H and ^{13}C NMR spectra were recorded on Bruker AC 300 or AM 400 spectrometers. Electrospray mass spectra (ES MS) were recorded on a Finnigan Mat LCT or LCQ mass spectrometer. Infrared spectra were recorded on a Shimadzu FTIR 8300 Fourier transform spectrophotometer with solid samples by use of a Golden Gate ATR. UV−Vis absorption spectra were recorded on a Hewlett-Packard 8453 diode-array spectrophotometer (polymer films) or a Shimadzu 3100 UV/Vis/NIR spectrophotometer (monomers). Spectra of polymer films were recorded by use of potentiodynamically deposited polymer films on Fluorine-Doped Tin Oxide (FDTO)-coated glass slides (Libbey-Owens-Ford, 8 Ω/square), which were immersed in an acetonitrile-filled 1 cm × 1 cm glass cuvette. All absorption spectra were recorded in acetonitrile (spectrophotometric grade). Cyclic voltammetry was carried out on a CH Instruments model 660A potentiostat or 900A bipotentiostat. In situ conductivity measurements were carried out on a CH Instruments 900A bipotentiostat with modified software. Platinum disk electrodes (2 mm diameter) sealed in Kel-F were purchased from CH Instruments. Platinum disk microelectrodes were manufactured by sealing platinum microwires (Goodfellow Metals Inc.) in soft glass by a previously described procedure.[11] Platinum interdigitated electrode arrays, IDAs, were purchased from Abtech Scientific. The IDA electrodes had 25 digit pairs, a digit width and interdigit gap width of 5 μm, and a digit height of 0.1 μm, and the digit length was 3 mm. Electrochemical measurements were carried out in a conventional three-electrode cell, with a coiled platinum wire or a Pt flag as the counterelectrode and an acetonitrile-filled double-junction Ag/Ag^+ (0.01 M $AgNO_3$ + 0.1 M [*n*-Bu_4N][BF_4]) half-cell as the reference electrode. The potential of this electrode was referenced externally versus that of the ferrocene/ferrocenium, Fc/Fc^+, couple. The solutions were degassed previous to measurements and maintained under a nitrogen or argon atmosphere throughout experiments. Poly-[Ru(ttpy)$_2$]$^{2+}$ and Poly-[Os(ttpy)$_2$]$^{2+}$ were deposited from BF_3·OEt_2 solutions. The other polymers were deposited from CH_3CN + BF_3·OEt_2 (95:5) solutions. Solution-phase electrochemistry was carried out in acetonitrile solutions of the complexes. Polymer film voltammetry and in situ dc conductivity measurements were carried out in CH_3CN + BF_3·OEt_2 (95:5) solutions, unless otherwise stated. In all cases 0.1 M [*n*-Bu_4N][BF_4] was added as supporting electrolyte. All electrodeposition was carried out potentiodynamically at scan rates of 50 or 100 mV s^{-1}.

Synthesis of [Ru(bttpy)$_2$][PF_6]$_2$. 4′-(2,2′-Bithien-5-yl)-2,2′:6′,2″-terpyridine (bttpy, 34.2 mg, 0.086 mmol) and $RuCl_3$·$3H_2O$ (8.5 mg, 0.033 mmol) were suspended in 10 mL of ethane-1,2-diol. After 4 drops of *N*-ethylmorpholine was added, the reaction mixture was heated in a microwave oven (600 W, 4 min) to give a red solution. The solution was cooled to room temperature and aqueous [NH_4][PF_6] was added. The precipitate was collected on Celite and redissolved in MeCN, and the solvent was removed in vacuo. The crude product was purified by column chromatography (SiO_2), first eluting with MeCN/saturated aqueous KNO_3/H_2O (7:1:0.5) and then with MeCN/saturated aqueous KNO_3/H_2O (7:2:2); the major red fraction was collected. The volume of solvent was reduced and aqueous [NH_4][PF_6] was added. The precipitate was collected over Celite and dissolved in MeCN, and the solvent was removed in vacuo to give [Ru(bttpy)$_2$][PF_6]$_2$ as a red solid (yield, 15.6 mg, 32%). ^{1}H NMR (CH_3CN, 400 MHz) δ 8.88 (H^{B3}, 4H, s), 8.64 (H^{A3}, 4H, d, J = 8.64 Hz), 8.12 (H^{C3}, 2H, d, J = 4.04 Hz), 7.94 (H^{A4}, 4H, dt, J = 1.47, 7.72 Hz), 7.54 (H^{C4}, 2H, d, J = 4.04 Hz), 7.50 (H^{D5}, 2H, dd, J = 1.10, 4.78 Hz), 7.49 (H^{D3}, 2H, dd, J = 1.10, 4.78 Hz), 7.43 (H^{A6}, 4H, d, J = 6.25 Hz), 7.18 (H^{D4}, 2H, d, J = 3.66, 5.14 Hz), 7.16 (H^{A5}, 4H, dt, J = 1.10, 7.35 Hz); ES MS *m*/*z* (calcd) 1040, [M − PF_6]$^+$); 448, [M − 2PF_6]$^{2+}$); IR (solid, cm^{-1}) 2923w, 1608m, 1554w, 1431m, 1369m, 1245m, 1161w, 1080m, 964w, 825s (PF_6), 783s, 752m, 698m, 648m, 621m, 555s (PF_6), 520s.

Synthesis of 2,2′:5′,2″-Terthiophene-5-carbaldehyde. 2,2′:5′,2″-Terthiophene (1.48 g, 6.00 mmol) and dry *N*,*N*-dimethylformamide (DMF) (0.513 mL, 7.0 mmol) dissolved in 10 mL of dry dichloroethane were cooled to 0 °C, and $POCl_3$ (0.616 mL, 6.60 mmol) was added slowly to give a green solution. The solution was heated at 60 °C for 3 h, during which time it turned red and some solid precipitated. The solution was cooled and then poured onto ice. After the ice had melted, the solution was neutralized with saturated aqueous NaOAc and a pale solid precipitated. The solid was collected and further product was extracted from the filtrate with chloroform. The product was purified by column chromatography (SiO_2, hexane/EtOAc 1:2). This gave two yellow bands; the first fraction showed a yellow luminescence under UV irradiation and was the desired aldehyde. The product was isolated as a yellow-green solid (yield, 1.52 g, 85%). ^{1}H NMR ($CDCl_3$, 400 MHz, ring numbering as for ligand tttpy) δ 9.89 (C*H*O, 1H, s), 7.71 (H^{C3}, 1H, d, J = 4.0 Hz), 7.32 (H^{E5}, 1H, dd, J = 1.1, 5.1 Hz), 7.30 (H^{C4}, 1H, d, J = 4.04 Hz), 7.27 (H^{D3}, 1H, d, J = 4.0 Hz), 7.26 (H^{E3}, 1H, dd, J = 1.0, 3.6 Hz), 7.16 (H^{D4}, 1H, d, J = 4.0

(8) Encinas, S.; Flamigni, L.; Barigelletti, F.; Constable, E. C.; Housecroft, C. E.; Schofield, E. R.; Figgemeier, E.; Fenske, D.; Neuburger, M.; Vos, J. G.; Zehnder, M. *Chem. Eur. J.* **2002**, *8*, 137.
(9) Constable, E. C.; Handel, R.; Housecroft, C. E.; Neuburger, M.; Schofield, E. R.; Zehnder, M. *Polyhedron* **2002**, *23*, 135.
(10) Hjelm, J.; Handel, R. W.; Hagfeldt, A.; Constable, E. C.; Housecroft, C. E.; Forster, R. J. *J. Phys. Chem. B* **2003**, *107*, 10431.
(11) Forster, R. J.; Faulkner, L. R. *J. Am. Chem. Soc.* **1994**, *116*, 5444.

Hz), 7.09 (H^{E4}, 1H, dd, J = 3.7, 5.1 Hz); ^{13}C NMR ($CDCl_3$, 100 MHz) δ 182.3 (CHO), 146.8 (C^{quat}), 141.6 (C^{quat}), 139.2 (C^{quat}), 137.3 (C^{C3}), 136.4 (C^{quat}), 134.4 (C^{quat}), 128.0 (C^{E4}), 126.8 (C^{D3}), 125.3 (C^{E5}), 124.6 (C^{D4}), 124.5 (C^{E3}), 124.0 (C^{C4}); EI MS *m*/*z* (calcd) 276 (276, $[M]^+$), 248 (247, $[M - CHO]^+$); IR (solid, cm^{-1}) 3062w, 2796w, 1647m, 1554w, 1504w, 1423m, 1377m, 1284w, 1218m, 1068m, 1045m, 983w, 898w, 867w, 833m, 790s, 748m, 705s, 663m, 617m, 513s.

Synthesis of 4′-(2,2′:5′,2″-Terthien-5-yl)-2,2′:6′,2″-terpyridine (tttpy). 2-Acetylpyridine (81 μL, 1.0 mmol) was added dropwise to a solution of K[^{t}BuO] (122 mg, 1.1 mmol) in 20 mL of dry THF. This was stirred at room temperature for 30 min to give a cream-yellow suspension. 2,2′:5′,2″-Terthiophene-5-carbaldehyde (100 mg, 0.4 mmol) in 10 mL of dry THF was then added. Almost immediately the solution turned clear brown. The solution was stirred overnight at room temperature, and then $[NH_4][OAc]$ (2.5 g, 0.032 mol) in 30 mL of EtOH/AcOH (2:1) was added and the reaction mixture was heated to reflux for 5 h. Thin-layer chromatography (TLC) on Al_2O_3 with toluene + 5% Et_2NH as eluent showed one band that stained green with $FeSO_4$ solution. The reaction mixture was cooled to room temperature and then poured onto ice. It was left for 3 h and a pale solid precipitate A was separated by filtration. The filtrate was extracted with $CHCl_3$ (3 × 20 mL) and removal of the organic solvent gave a brown oil B. TLC of A indicated pure product; B showed side products and was purified on a column, (Al_2O_3, toluene + 5% Et_2NH). Yield: bright yellow solid, A 11.9 mg, B 67.0 mg (overall 83%). ^{1}H NMR ($CDCl_3$, 300 MHz): δ 8.74 (H^{A6}, 2H, d, J = 4.8 Hz), 8.64 (H^{B3}, 2H, s), 8.62 (H^{A3}, 2H, d, J = 7.7 Hz), 7.86 (H^{A4}, 2H, dt, J = 1.83, 7.7 Hz), 7.68 (H^{C3}, 1H, d, J = 4.0 Hz), 7.34 (H^{A5}, 2H, ddd, J = 1.10, 4.8, 7.3 Hz), 7.22 (H^{E5}, 1H, d, J = 4.8 Hz), 7.19 (H^{C4}, 1H, d, J = 3.8 Hz), 7.18 (H^{E3}, 1H, d, J = 3.7 Hz), 7.14 (H^{D3}, 1H, d, J = 4.0 Hz), 7.08 (H^{D4}, 1H, d, J = 4.0 Hz), 7.01 (H^{E4}, 1H, dd, J = 3.7, 4.8 Hz); ^{13}C NMR ($CDCl_3$, 100 MHz) δ 155.9 (C^{B2}), 155.8 (C^{A2}), 149.0 (C^{A6}), 142.9 (C^{B4}), 140.2 ($C^{quat,thiophene}$), 138.7 ($C^{quat,thiophene}$), 136.9 (C^{A4}/ $C^{quat,thiophene}$), 136.9 ($C^{quat,thiophene}$), 135.7 ($C^{quat,thiophene}$), 127.9 (C^{E4}), 126.7 (C^{C3}), 124.8 (C^{D3}), 124.6 (C^{E5}), 124.5 (C^{C4}), 124.4 (C^{D4}), 123.9 (C^{A5}), 123.8 (C^{E3}), 121.3 (C^{A3}), 116.6 (C^{B3}); ES MS *m*/*z* (calcd) 480 (480, $[M + H]^+$), 502 (502, $[M + Na]^+$); HRMS $C_{27}H_{18}N_3S_3$ $[M + H^+]$ 480.066, found 480.065; IR (solid, cm^{-1}) 3062w, 2923w, 2854w, 1735w, 1581m, 1458m, 1396m, 1226m, 1157w, 1041w, 987w, 871w, 833w, 783s, 725m, 617w, 516s; mp 185−190°C.

Synthesis of [Os(tttpy)$_2$][PF$_6$]$_2$. A mixture of 4′-(2,2′:5′,2″-terthien-5-yl)-2,2′:6′,2″-terpyridine (66.6 mg, 0.14 mmol) and $K_2[OsCl_6]$ (22 mg, 0.046 mmol) was suspended in 10 mL of ethane-1,2-diol with 5 drops of *N*-ethylmorpholine. The reaction mixture was heated in a microwave oven (600 W, 4 min) to give a clear brown solution. Another portion of $K_2[OsCl_6]$ (19 mg, 0.040 mmol) was added, and the reaction mixture was heated for another 4 min. The crude product was purified by column chromatography (SiO_2, MeCN/saturated aqueous KNO_3/H_2O 7:1:0.5). Two brown bands were separated, but NMR spectroscopic characterization indicated the presence of a mixture of products in each fraction. Preparative TLC of the crude product gave several bands, of which the main brown band was collected; this was further purified by HPLC. The final product was precipitated as a brown solid by adding aqueous $[NH_4][PF_6]$ (yield 27.2 mg, 27%). ^{1}H NMR (CD_3CN, 400 MHz) δ 8.90 (H^{B3}, 4H, s), 8.62 (H^{A3}, 4H, d, J = 7.7 Hz), 8.04 (H^{C3}, 2H, d, J = 4.0 Hz), 7.80 (H^{A4}, 4H, dt, J = 1.5, 7.7 Hz), 7.55 (H^{C4}, 2H, d, J = 4.0 Hz), 7.42−7.39 ($H^{D3/E5}$, 4H, m), 7.35−7.33 ($H^{D4/E3}$, 4H, m), 7.28 (H^{A6}, 4H, d, J = 4.8 Hz), 7.11 (H^{A5}, 4H, m), 7.08 (H^{E4}, 2H, m); ES MS *m*/*z* (calcd) 1461 (1461, $[M + Na]^+$), 1295 (1294, $[M - PF_6]^+$), 575 (574, $[M - 2PF_6]^{2+}$).

Results and Discussion

Synthesis and Characterization. The syntheses of the ligands 4′-(2-thienyl)-2,2′:6′,2″-terpyridine (ttpy, Chart 1) and 4′-[5-(2,2′-bithien-5-yl]-2,2′:6′,2″-terpyridine (bttpy, Chart 1) and of the complexes $[Os(ttpy)_2]^{2+}$, $[Ru(ttpy)_2]^{2+}$, and $[Os(bttpy)_2]^{2+}$ have been described previously.[8−10] The complex $[Ru(bttpy)_2][PF_6]_2$ was prepared by the reaction of $RuCl_3 \cdot 3H_2O$ with bttpy in ethane-1,2-diol under reducing conditions (*N*-ethylmorpholine) in a modified microwave oven. The highest mass peaks in the electrospray mass spectrum of the complex were at *m*/*z* 1040 and 448, corresponding to the molecular ions $[M - PF_6]^+$ and $[M - 2PF_6]^{2+}$, respectively; isotope distributions matched those calculated. In the ^{1}H NMR spectrum, signals assigned to protons in the tpy domain closely matched those of $[Ru(ttpy)_2][PF_6]_2$,[8,9] and the spectrum as a whole resembled that of $[Os(bttpy)_2][PF_6]_2$;[10] all signals were assigned by correlated spectroscopic (COSY) techniques.

The one-pot synthesis of bttpy from 2,2′-bithiophene-5-carbaldehyde and 2-acetalpyridine that we reported previously[10] has now been extended to the more highly conjugated derivative 4′-(2,2′:5′,2″-terthien-5-yl)-2,2′:6′,2″-terpyridine, tttpy. This ligand was prepared in 85% yield by the reaction of 2,2′:5′,2″-terthiophene-5-carbaldehyde and 2-acetalpyridine in the presence of K[^{t}BuO] in THF, followed by treatment with NH_4OAc in EtOH/AcOH. The ligand was stored in the dark as it slowly decomposed on exposure to light. The electrospray MS showed a parent ion for $[M + H]^+$ at *m*/*z* 480 in addition to a peak at *m*/*z* 502 assigned to $[M + Na]^+$; a high-resolution mass spectrum also confirmed the composition of the ligand. In the ^{1}H NMR spectrum of tttpy, signals assigned to the tpy part of the ligand were readily assigned by COSY techniques and were reminiscent of those for the related bttpy and ttpy ligands.[8−10] While the doublet for proton H^{C3} was well-resolved at δ 7.68, signals for the remaining thiophene protons appeared in the region δ 7.5−7.0 with significant overlapping of peaks. Unambiguous assignments (see Experimental Section) were made from nuclear Overhauser effect (nOe) experiments at 500 MHz. The ^{13}C NMR spectrum of tttpy was assigned by comparing the spectrum with those of bttpy and ttpy and with the aid of DEPT and HETCOR measurements; the signals for the thiophene quaternary C atoms were not individually assigned.

The complex $[Os(tttpy)_2][PF_6]_2$ was prepared by an analogous method used for the synthesis of $[Os(bttpy)_2][PF_6]_2$.[10] Purification of $[Os(tttpy)_2][PF_6]_2$ proved difficult, even by HPLC methods. In the electrospray mass spectrum of $[Os(tttpy)_2][PF_6]_2$, peaks at *m*/*z* 1461, 1295, and 575 were assigned to the ions $[M + Na]^+$, $[M - PF_6]^+$, and $[M - 2PF_6]^{2+}$, respectively, and showed appropriate isotopic distributions. Signals assigned to the tpy protons in the ^{1}H NMR spectrum of $[Os(tttpy)_2][PF_6]_2$ closely resembled those of $[Os(bttpy)_2][PF_6]_2$ and were readily assigned. As for the free ligand, significant overlapping of signals for the

Table 1

complex or polymer	m	reductions[a] (V vs Fc/Fc^+)	oxidations[a] (V vs Fc/Fc^+)	λ_{max}, ^{1}MLCT (nm) [λ_{max}, ^{3}MLCT (nm)]
$[Os(tpy)_2]^{2+}$ [b]	0	−1.89, −1.60	+0.54,[c] +1.60[d,e]	475 [656]
$[Ru(tpy)_2]^{2+}$ [b]	0	−1.90, −1.65	+0.89[c]	475
$[Os(ttpy)_2]^{2+}$	1	−1.81, −1.56	+0.49,[c] +1.45,[d] +1.77[d,e]	498 [674]
$[Os(bttpy)_2]^{2+}$	2	nd	+0.48,[c] +0.99[d]	513 [682]
$[Os(tttpy)_2]^{2+}$	3	nd	+0.49,[c] +0.77[d]	514 [682]
$[Ru(ttpy)_2]^{2+}$	1	−1.83, −1.59	+0.82,[c] +1.65[d]	498
$[Ru(bttpy)_2]^{2+}$	2	−1.79, −1.57	+0.84[d,f]	514
poly$[Os(ttpy)_2]^{2+}$	1	−1.84, −1.52	+0.56,[c] nd	nd
poly$[Os(bttpy)_2]^{2+}$	2	−1.74, −1.46	+0.52,[c] +0.74, +1.05	530 [692]
poly$[Os(tttpy)_2]^{2+}$	3	nd, −1.53	+0.4, +0.57,[c] +0.8	nd
poly$[Ru(ttpy)_2]^{2+}$	1	−1.77, −1.56	+0.91,[c] +1.36	528
poly$[Ru(bttpy)_2]^{2+}$	2	nd, −1.49	+0.64, +0.88,[c] +1.15	538

[a] The potentials given for reversible redox couples of complexes in solution are half-wave potentials, $E_{1/2}$, taken as $(E_{pa} + E_{pc})/2$ and were measured in acetonitrile containing 0.1 M $[n\text{-}Bu_4N][BF_4]$ as supporting electrolyte. The redox potentials given for the polymers were measured at slow scan rates (exhaustive bulk electrolysis conditions) in monomer free electrolyte and thus are formal potentials, $E^{\circ\prime}$, also taken as $(E_{pa} + E_{pc})/2$. All polymer potentials refer to polymer films deposited on Pt electrodes. [b] UV−Vis data taken from ref 8. Electrochemical data were measured under the same conditions as for the thienyl-substituted complexes (footnote *a*). [c] Metal-centered redox couple. [d] Irreversible wave; the potential given is the anodic peak potential, E_{pa}. [e] Os(III/IV) redox wave; see refs 39−41. [f] Ru(III/II) wave overlapped with ligand oxidation waves; could not be separated by differential pulse voltammetry.

thiophene protons was observed and assignments were made by use of COSY and nOe experiments.

UV−Visible Spectroscopy. UV−visible spectroscopy represents a powerful approach to elucidating the effect of increased conjugation length on the separation between the highest occupied and lowest unoccupied molecular orbitals. Table 1 contains information about the wavelengths of maximum absorbance for the monomers and polymers investigated. The ruthenium monomers all display the characteristic singlet−singlet metal-to-ligand charge transfer (^{1}MLCT) band typical of $\{Ru(tpy)_2\}$ complexes. The Os monomers display both a ^{1}MLCT band and a less intense spin-forbidden singlet−triplet transition (^{3}MLCT) at longer wavelengths, which is typical of an $[Os(Xtpy)_2]^{2+}$ system with high spin−orbit coupling. All monomers display ligand-centered transitions at shorter wavelengths (in the interval 320−400 nm), which are located at successively lower energies for the monomers with bithienyl and terthienyl substituents. Significantly, consistent with an increased conjugation length, the MLCT bands shift to lower energy as the number of thienyl groups in the bridge increases. Moreover, the sensitivity of the position of the MLCT band to polymerization indicates that it provides a useful insight into changes in the extent of conjugation around the metal centers, for example, changes triggered by electrochemical coupling.

Solution-Phase Electrochemical Properties. One of the key requirements of a model system for elucidating the effects of bridge-redox center resonance on the overall rate of charge transport is that the redox processes be electrochemically reversible at accessible time scales. Table 1 summarizes the half-wave potentials for the complexes dissolved in acetonitrile solution. The complexes all display metal-based oxidation waves when dissolved in solution, and the assignments of the redox processes have been made by reference to the known behavior[8,12] of $[Os(tpy)_2]^{2+}$ and $[Ru(tpy)_2]^{2+}$. With the exception of $[Ru(bttpy)_2]^{2+}$ these redox processes are electrochemically reversible and display peak-to-peak separations of less than 90 mV at a scan rate of 100 mV s^{-1}. The response observed for $[Ru(bttpy)_2]^{2+}$ is more complex with the ligand and metal oxidation waves centered at +0.84 V overlapping significantly. A lower metal-based oxidation potential is observed for the substituted complexes compared to the corresponding terpyridine-based model complex, which is consistent with the electron donation from the thiophene substituent. As expected, the ligand-based oxidation wave appears at successively lower potentials for complexes substituted with thiophene, bithiophene, and terthiophene, respectively. The ligand-based reductions appear at slightly less negative potentials than those of the $[Os(tpy)_2]^{2+}$ and $[Ru(tpy)_2]^{2+}$ parent complexes, most likely reflecting the increased ability of the extended conjugated system in the thienyl-substituted ligands to accommodate a higher charge density.

Solvent Effects on Electropolymerization. Polythiophene is known to display a 95%+ preference for α,α-coupling over α,β-coupling when it is synthesized electrochemically.[13] The oxidative electropolymerization of the homoleptic oligothienyl-substituted complexes is expected to result in the formation of linear polymers with the α-carbons of the outermost thienyl groups of each complex linked to the neighboring complexes' outermost α-carbons. As illustrated in Scheme 1, this coupling scheme is expected to give rise to polymers where the $\{M(tpy)_2\}$ moieties are linked by two, four, or six thienyl groups. Previously, we reported X-ray photoelectron spectroscopic (XPS) and UV−vis data which suggested that poly$[Ru(ttpy)_2]^{2+}$ is mainly α,α-coupled.[14]

Figure 1 illustrates the potentiodynamic electropolymerization of $[Ru(ttpy)_2]^{2+}$, $[Os(bttpy)_2]^{2+}$, $[Ru(bttpy)_2]^{2+}$, and $[Os(tttpy)_2]^{2+}$. The peak currents in each case increase with each scan, indicating the accumulation of an electroactive film on the electrode surface. After rinsing of the electrodes with acetone and acetonitrile, a deep red film of insoluble material is observed on the surface of the electrode. An important aspect influencing electropolymerization in these systems is the stability of the electrogenerated cation radical. The cation radicals of the ttpy ligand are the least stable, and experimentally one observes that complexes $[Os(ttpy)_2]^{2+}$

(12) Constable, E. C.; Cargill Thompson, A. M. W.; Tocher, D. A.; Daniels, M. A. M. *New J. Chem.* **1992**, *16*, 855.
(13) Roncali, J. *Chem. Rev.* **1992**, *92*, 711.
(14) Hjelm, J.; Constable, E. C.; Figgemeier, E.; Hagfeldt, A.; Handel, R.; Housecroft, C. E.; Mukhtar, E.; Schofield, E. *Chem. Commun.* **2002**, 284.

Scheme 1. Proposed Structure of the Electrochemically Synthesized Polymers

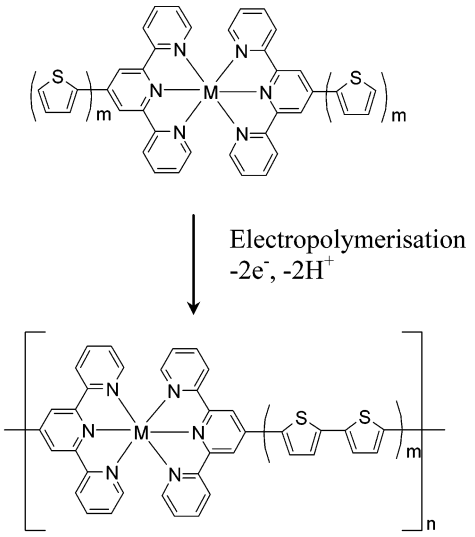

Ligands:	Metals (M):
m = 1 ⇔ ttpy	Ru(II), Os(II)
m = 2 ⇔ bttpy	Ru(II), Os(II)
m = 3 ⇔ tttpy	- , Os(II)

and $[Ru(ttpy)_2]^{2+}$ require rigorous exclusion of water and other nucleophilic impurities for successful electropolymerization. Moreover, these complexes have the highest onset potentials for polymerization. Here, to ensure efficient electropolymerization and the formation of a conducting polymer film, the polymerization of $[Os(ttpy)_2]^{2+}$ and $[Ru(ttpy)_2]^{2+}$ was performed in electrolyte solutions where $BF_3{\cdot}OEt_2$ was used as solvent.[15−18] Significantly, indistinguishable electrochemical properties are observed for films of poly$[Ru(ttpy)_2]^{2+}$ films synthesized in $BF_3{\cdot}OEt_2$ and CH_2Cl_2, suggesting that the solvent influences the lifetime of the cation radical rather than the film structure. The $[Os(ttpy)_2]^{2+}$ complex forms only very thin polymer films ($[\Gamma = (1-2) \times 10^{-9}$ mol cm^{-2}, 10−20 monolayer equivalents] when electropolymerized from $BF_3{\cdot}OEt_2$, while it is possible to form polymer films of up to apparent surface coverages of

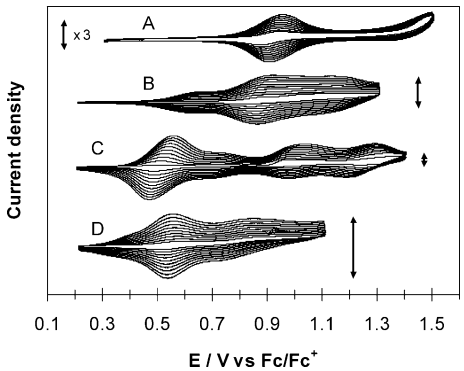

Figure 1. Oxidative electropolymerization of oligothienyl-substituted complexes onto Pt disk electrodes. The bars indicate a current density of 1 mA cm^{-2}. The scan rate was 0.1 V s^{-1} in all cases. The solutions were saturated with monomer, unless otherwise stated. (A) Poly$[Ru(ttpy)_2]^{2+}$; (B) poly$[Ru(bttpy)_2]^{2+}$; (C) poly$[Os(bttpy)_2]^{2+}$ deposition from a 0.4 mM solution of the monomer; (D) poly$[Os(tttpy)_2]^{2+}$.

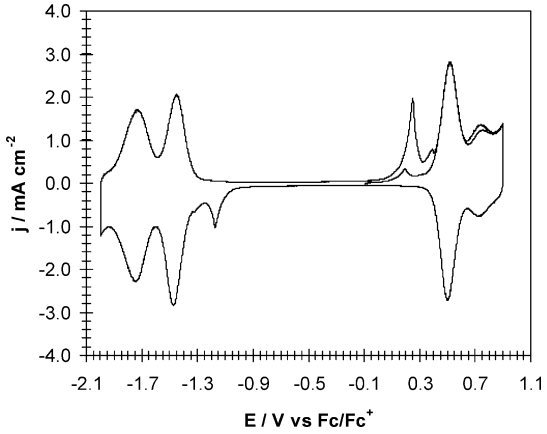

Figure 2. Cyclic voltammogram of a thin film of poly$[Os(bttpy)_2]^{2+}$ deposited on a 50 μm radius Pt disk electrode ($\Gamma = 1.1 \times 10^{-9}$ mol cm^{-2}) at 0.5 V s^{-1} in CH_3CN containing 0.1 M [n-Bu_4N][BF_4] as supporting electrolyte.

5×10^{-8} mol cm^{-2} of the complex $[Ru(ttpy)_2]^{2+}$. This difference in polymerization efficiency cannot be explained alone by the different separation in energy of the metal- and bridge-based redox processes ($\Delta E_{bridge-M}$) in the two materials. As both the metal centers and the bridges in either material should be able to independently mediate the oxidation of the ligand necessary for film growth, by intra- and interstrand electron hopping, this result may reflect the impact of differences in the radical lifetime, partial overoxidation, and differences in conductivity on polymer growth kinetics. In a later section we address the influence of $\Delta E_{bridge-M}$ on the charge transport dynamics in greater detail.

In contrast to the ttpy systems, electropolymerized films of $[Os(bttpy)_2]^{2+}$ and $[Ru(bttpy)_2]^{2+}$ can be easily prepared in acetonitrile-based solutions even in the absence of added Lewis acid. However, addition of $BF_3{\cdot}OEt_2$ increases the polymerization efficiency significantly, and polymerization occurs for switching potentials up to +1.4 V.[19] The presence of the Lewis acid dramatically increases the electrochemical reversibility of the thienyl-based redox waves during electropolymerization, and very thick polymer films could be grown ($\Gamma > 1 \times 10^{-6}$ mol cm^{-2}).

Voltammetry of Polymer Films. The voltammetry of polymer films has been explored in CH_3CN containing 0.1 M [n-Bu_4N][BF_4] as supporting electrolyte that does not contain any monomer. Figure 2 illustrates the voltammetry of a poly$[Os(bttpy)_2]^{2+}$-coated Pt electrode, where the potential is scanned through both the polymer reductions and the first two oxidations, for example, a metal-centered and a quaterthienyl-centered oxidation process. The sharp irreversible peaks before the oxidation and reduction waves are observed for all polymers when the potential is scanned through both oxidation and reduction processes in the same scan, irrespective of the initial scan direction. If the potential

(15) Jin, S.; Xue, G. *Macromolecules* **1997**, *30*, 5753.
(16) Zhang, D.; Qin, J.; Xue, G. *Synth. Met.* **1999**, *106*, 161.
(17) Shi, G.; Li, C.; Liang, Y. *Adv. Mater.* **1999**, *11*, 1145.
(18) Li, C.; Shi, G.; Liang, Y. *J. Electroanal. Chem.* **1998**, *455*, 1.
(19) For a more detailed study on the electropolymerization dynamics, see Hjelm, J.; Handel, R. W.; Hagfeldt, A.; Constable, E. C.; Housecroft, C. E.; Forster, R. J. *Electrochem. Commun.* **2004**, *6*, 193.

is scanned in one direction first (anodic or cathodic) and subsequently scanned repeatedly only in the opposite (reduction or oxidation) region, the sharp peak appears on the first scan but is diminished over the following scans. This behavior is also independent of the initial scan direction. This phenomenon is referred to as charge trapping and was first observed for spatially segregated bilayer redox-active films.[20,21] Charge trapping has since been observed for numerous homogeneous single- and multicomponent redox-active films.[22−26] The charge trapping peaks observed are attributed to the presence of redox centers who are electronically isolated from the electrode surface, so that their redox current is mediated by adjacent redox centers in a manner similar to that of bilayer films.

Table 1 summarizes the measured redox potentials for the polymers and shows that the polymers are reduced at slightly less negative potentials than the corresponding monomers. This behavior is entirely consistent with an increased conjugation length in the polymers.

Since the oligothienyl-based oxidations were unstable where the solvent is pure CH_3CN, the anodic electrochemistry of the polymers deposited on platinum electrodes was investigated in monomer-free CH_3CN containing 5% $BF_3 \cdot OEt_2$. Under these conditions, the extent of polymer degradation caused by oxidation of the thienyl bridges is negligible.

The electrosynthesized polymers display both metal- and bridge-based redox waves, respectively, in the anodic range. The first bridge-based redox process of the polymers occurs at a significantly lower potential than the onset potential of monomer ligand oxidation, indicating an increase of the conjugation upon electrochemical coupling. The $\Delta E_{\text{bridge}-\text{M}}$ values for the polymers are in the range +450 mV down to −240 mV and decrease as the number of thienyl units in the bridges of the polymers increase. In the following section the dc conductivity of two quaterthienyl-bridged polymers with different $\Delta E_{\text{bridge}-\text{M}}$ values is examined.

In Situ Conductivity. Quaterthienyl-bridged polymers were successfully deposited onto interdigitated platinum microelectrode arrays, IDAs, from acidified acetonitrile solutions. The IDAs were coated potentiodynamically (at 50 mV s^{-1}) with polymer films, in such a manner that the interdigit gaps were bridged by a continuous polymer film. Dc conductivity measurements were carried out in monomer free electrolyte by the method developed by Wrighton and co-workers.[27−30] A small potential difference, E_{offset}, was applied between the two electrodes (typically 20 mV), after which the electrodes were scanned at a slow scan rate (5 mV s^{-1}) while maintaining the potential difference. The drain current, i_D, that flows between the two electrodes can be related directly to the film conductivity, σ_{film}. Ohm's law is used to calculate the total measured resistance, R_{film}. The film conductivity was calculated by multiplying $(1/R_{\text{film}})$ with the so-called Zaretsky cell constant, K_Z ($K_Z = 0.13$ cm^{-1} for all IDAs used here), which yields the film conductivity.[31,32] The correlation between the theoretical values of K_Z has been found to agree with experimental data for different arrays in a study where the conductivity was measured by impedance spectroscopy of the arrays immersed in electrolyte solutions.[31] To obtain the absolute film conductivity, one needs to either know the film thickness or grow it so thick that the conductivity is probed entirely inside the material. However, no reliable measurements of the film thickness could be obtained by atomic force microscopy (AFM) or step profilometry. Instead, we chose to adopt an approach similar to that used by Zotti and co-workers for conductivity measurements on dual microband electrodes.[33] The conductivity measurements were carried out on polymer films that were grown sufficiently thick to completely fill up the gaps between the digits of the array. The drain current was monitored during the coating procedure by maintaining a small potential offset between the two sets of electrodes. As illustrated in Figure 3, the drain current increases rapidly during the first few scans but levels off rapidly after 5−10 scans and a drain current plateau is observed in a plot of drain current vs deposition scan number. The drain current increase with each scan as the interdigit gap is successively filled up with polymer. The electrodes were washed with

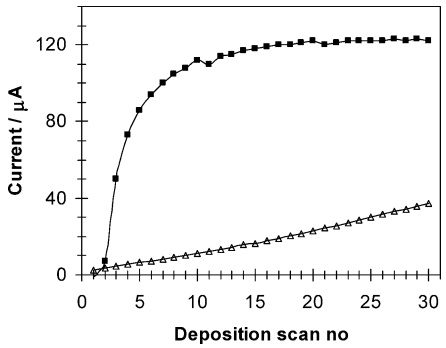

Figure 3. Plot of the drain current (monitored at +1.04 V) vs deposition scan number during the potentiodynamic electrodeposition of poly[Ru(bttpy)$_2$]$^{2+}$ onto a Pt IDA (■) from a 0.4 mM solution of the monomer. The scan rate was 0.05 V s^{-1}, the offset voltage was 20 mV, and the anodic switching potential was +1.1 V. (△) Polymer film electrolysis current during electrodeposition of poly[Ru(bttpy)$_2$]$^{2+}$ monitored at +1.04 V, by use of a Pt IDA of the same dimensions, when both electrodes are scanned together under the same conditions.

(20) Abruña, H. D.; Denisevich, P.; Umaña, M.; Meyer, T. J.; Murray, R. W. *J. Am. Chem. Soc.* **1981**, *103*, 1.
(21) Denisevich, P.; Willman, K. W.; Murray, R. W. *J. Am. Chem. Soc.* **1981**, *103*, 4727.
(22) Takada, K.; Storrier, G. D.; Pariente, F.; Abruña, H. D. *J. Phys. Chem. B* **1998**, *102*, 1387.
(23) Cameron, C. G.; Pickup, P. G. *J. Am. Chem. Soc.* **1999**, *121*, 11773.
(24) Guarr, T. F.; Anson, F. C. *J. Phys. Chem.* **1987**, *91*, 4037.
(25) Willman, K. W.; Murray, R. W. *J. Electroanal. Chem.* **1982**, *133*, 211.
(26) Bernhard, S.; Takada, K.; Díaz, D. J.; Abruña, H. D.; Mürner, H. *J. Am. Chem. Soc.* **2001**, *123*, 10265.
(27) Paul, E. W.; Ricco, A. J.; Wrighton, M. S. *J. Phys. Chem.* **1985**, *89*, 1441.
(28) Kittlesen, G. P.; White, H. S.; Wrighton, M. S. *J. Am. Chem. Soc.* **1984**, *106*, 7389.
(29) Ofer, D.; Crooks, R. M.; Wrighton, M. S. *J. Am. Chem. Soc.* **1990**, *112*, 7869.
(30) Thackeray, J. W.; White, H. S.; Wrighton, M. S. *J. Phys. Chem.* **1985**, *89*, 5133.
(31) Sheppard, N. F.; Tucker, R. C.; Wu, C. *Anal. Chem.* **1993**, *65*, 1199.
(32) Guiseppi-Elie, A. *Measuring Electrical Materials Properties Using Microfabricated Interdigitated Microsensor Electrodes and Independently Adressable Microband Electrodes*; Abtech Scientific, Inc. application note.
(33) Schiavon, G.; Sitran, S.; Zotti, G. *Synth. Met.* **1989**, *32*, 209.

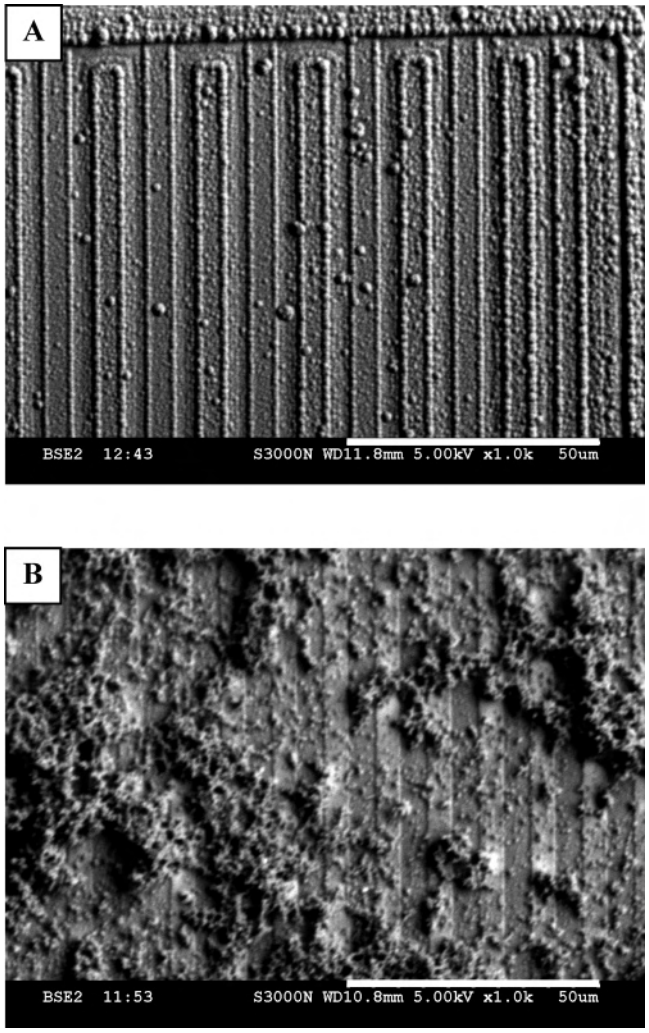

Figure 4. SEM images of polymer-coated Pt IDAs (5 μm digit width; 5 μm interdigit gaps) used for limiting conductivity measurements: (A) poly-[Os(bttpy)$_2$]$^{2+}$-coated IDA; (B) poly[Ru(bttpy)$_2$]$^{2+}$-coated IDA.

acetonitrile, and the total resistance of each coated array, R_{total}, was then measured in fresh monomer-free electrolyte at a scan rate of 5 mV s^{-1}. The drain current measured in this way in monomer-free electrolyte was within 5% of that observed at the plateau in the plot in Figure 3. Note that the electrolysis current is increasing continuously during the deposition experiment, indicating a continuously increasing film thickness throughout the experiment, while the drain current reaches a limiting value. This limiting drain current was taken as a measure of the absolute conductivity of the polymer, and the conductivities obtained in this way allow comparison between different polymers. The films used for limiting conductivity measurements were grown using the same switching potential ($E_{switch} = +1.1$ V).

Figure 4 panels A and B show SEM images of Os and Ru quaterthienyl-bridged polymer films, respectively, deposited on an IDA. This figure reveals that the two films exhibit radically different morphologies, suggesting that the nucleation and growth dynamics between the two quaterthienyl-bridged materials may differ significantly.

To accurately determine the film conductivity of highly conducting materials, it is necessary to ensure that the IDA

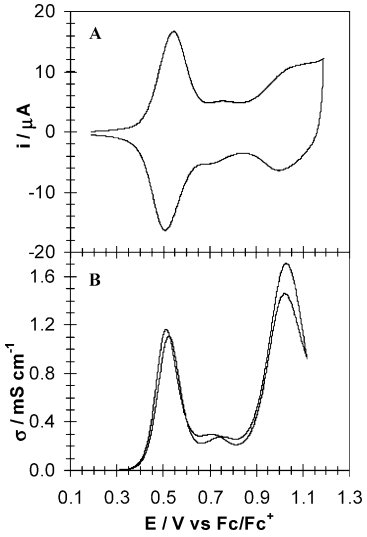

Figure 5. (A) Cyclic voltammogram of poly[Os(bttpy)$_2$]$^{2+}$-coated Pt IDA recorded at 0.05 V s^{-1}. (B) In situ conductivity profile of poly[Os(bttpy)$_2$]$^{2+}$-coated Pt IDA at 5 mV s^{-1} under the same conditions. Both forward and backward scans are shown. The offset voltage was 20 mV.

resistance does not contribute significantly to the overall cell resistance. For example, a film with a conductivity of 3 S cm^{-1} will contribute less than 0.05Ω to the overall measured resistance. Therefore, the on-chip resistance was determined by coating the IDAs with films of a highly conducting polymer (polybithiophene, 3 S cm^{-1})[34] and subsequently measuring R_{total}. The on-chip resistance determined from these measurements was 85(±1) Ω for the 3 mm long Pt IDAs used, which had 5 μm wide bands and 5 μm interdigit gaps.[35] This means that the upper conductivity limit that can be measured where the film resistance contributes at least 20% of total measured resistance is approximately 5×10^{-3} S cm^{-1}.

The quaterthienyl-bridged {Os(tpy)$_2$} and {Ru(tpy)$_2$} polymers investigated here display $\Delta E_{bridge-M}$ values of +220 and −240 mV, respectively. Figure 5A illustrates the anodic voltammetry of a poly[Os(bttpy)$_2$]$^{2+}$ film deposited on a Pt disk electrode. As illustrated in Figure 5B, the maximum conductivity occurs at the formal potential of each redox process, a typical observation for the dc conductivity of redox polymers.[7,36] The dc conductivity of the first thienyl bridge-based redox process in each material is significantly lower than that of the metal-based and the second thienyl bridge-based redox processes. In poly{Os(bttpy)$_2$} the ratio of the dc conductivity of the first and second bridge-based processes is 0.2, whereas it is 1 order of magnitude lower (0.02) for poly{Ru(bttpy)$_2$}. This observation likely reflects that there is a difference between the two materials in one or more of the intra- and interstrand electron exchange pathways that

(34) Zotti, G.; Schiavon, G. *Synth. Met.* **1990**, *39*, 183.
(35) The on-chip resistance was also measured by coating the digits and gaps of an IDA with silver paint, which was allowed to dry. The DC conductivity of the IDA plus leads was then measured with a multimeter and was determined to 65 Ω. Since the silver paint layer was much thicker than the digit height, this way of determining the on-chip resistance probably shorts out any resistance contribution from the Pt digits of the IDA, and the on-chip resistance determined by use of poly-bithiophene films was therefore considered more accurate.
(36) Chidsey, C. E. D.; Murray, R. W. *J. Phys. Chem.* **1986**, *90*, 1479.

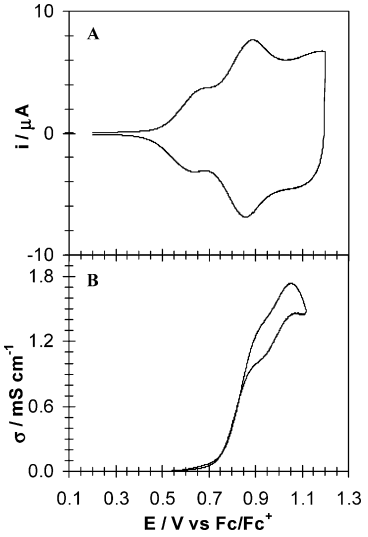

Figure 6. (A) Cyclic voltammogram of poly[Ru(bttpy)$_2$]$^{2+}$-coated Pt IDA recorded at 0.1 V s^{-1}. (B) In situ conductivity profile of poly[Ru(bttpy)$_2$]$^{2+}$-coated Pt IDA under the same conditions. Both forward and backward scans are shown. The offset voltage was 20 mV.

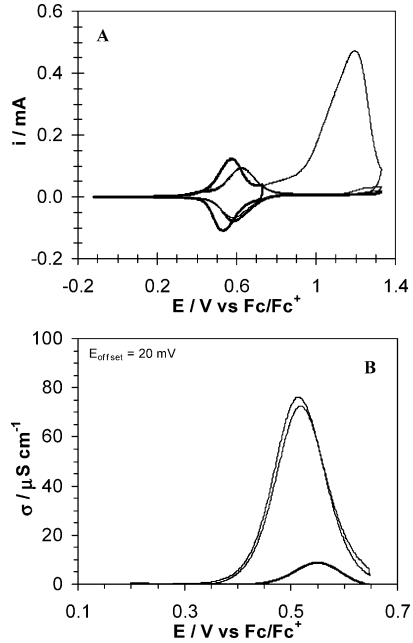

Figure 7. (A) Cyclic voltammogram of poly[Os(bttpy)$_2$]$^{2+}$-coated Pt wire electrode in CH_3CN containing 0.1 M [*n*-Bu_4N][BF_4] at 0.02 V s^{-1}. (B) In situ conductivity profile of a poly[Os(bttpy)$_2$]$^{2+}$ (thin film) coated Pt IDA in the same electrolyte at 5 mV s^{-1}. Both forward and backward scans are shown. The thick line is the in situ conductivity profile after partial overoxidation. The offset voltage was 20 mV.

are likely to govern the overall charge transport rate in the material. Somewhat simplified, the most immediate difference is the fact that the first bridge-based redox state in the Os polymer is surrounded by oxidized metal centers, where the Os centers could mediate sequential electron hopping between the bridge states, whereas in the Ru polymer, the first bridge-based redox state is surrounded by reduced Ru centers that cannot act as mediators.

Figure 6A illustrates the anodic voltammetry of poly[Ru(bttpy)$_2$]$^{2+}$. The redox process attributed to the Ru$^{2+/3+}$ couple, at +0.88 V, and to the second bridge-based redox couple, at about +1.15 V, are overlapped and are main contributors to the observed dc conductivity. The measured maximum conductivity of the quaterthienyl-bridged polymers is $1.6 \pm 0.3 \times 10^{-3}$ S cm^{-1} for the bridge-based couple irrespective of the identity of the metal center. Significantly, the conductivities obtained here for the metal-based processes are 2 orders of magnitude higher than that observed for the related nonconjugated system poly[Os(bpy)$_2$(vpy)$_2$]$^{2+}$, where vpy is 4-vinylpyridine.[36] This result indicates that charge transport rates can be significantly enhanced by matching of redox potentials of metal center and bridge states and by using conjugated bridges. The maximum conductivities obtained here are virtually identical to those reported previously by Swager and co-workers for quaterthienyl-bridged {Ru(bpy)$_3$} polymers,[37] materials that display very similar $\Delta E_{\text{bridge}-\text{M}}$ values.

Conductivity of Nonconjugated Materials. One distinct advantage of these novel materials is that the bridges can be overoxidized, leading to loss of conjugation. This switch allows the film conductivity to be measured for both conjugated and nonconjugated bridges *without* changing key parameters such as the concentration of redox centers within the film, local microenvironments etc. The bridge-based redox waves are not stable at elevated potentials ($E \geq +0.85$ V) in the absence of added acid, and the thienyl bridges are irreversibly oxidized. For example, Figure 7A shows that repeated scanning to elevated potentials leads to a collapse of the bridge-based redox waves within poly[Os(bttpy)$_2$]$^{2+}$ films. Overoxidation is expected to lead to a significant decrease in the extent of conjugation of the thienyl bridges[38] and is reflected in a shift of the MLCT band to higher energies following overoxidation of the films. Significantly, the integrated charge under the Os$^{2+/3+}$ wave remains constant, indicating that the {Os(tpy)$_2$} centers are left intact. However, the formal potential is shifted in a positive potential direction reflecting the weaker electron-donating ability of the nonconjugated quaterthienyl bridges after overoxidation. Figure 7B illustrates the dc conductivity of thin film of poly[Os(bttpy)$_2$]$^{2+}$ at 5 mV s^{-1} in acetonitrile containing 0.1 M [*n*-Bu_4N][BF_4] before and after overoxidation. The drain current, i.e., conductivity, drops by an order of magnitude when the material is overoxidized. This result highlights the importance of the conjugated bridges for the high redox conductivity observed in these materials.

Conclusions

A novel ligand, 4′-(2,2′:5′,2″-terthien-5-yl)-2,2′:6′,2″-terpyridine, and two new complexes were synthesized. From a series of homoleptic thienyl-, bithienyl-, and terthienyl-substituted tpy complexes, rodlike electroactive insoluble polymers were electrosynthesized from $BF_3{\cdot}OEt_2$, or CH_3CN

(37) Zhu, S. S.; Kingsborough, R. P.; Swager, T. M. *J. Mater. Chem.* **1999**, *9*, 2123.
(38) Pud, A. A. *Synth. Met.* **1994**, *66*, 1.
(39) Kober, E. M.; Caspar, J. V.; Sullivan, B. P.; Meyer, T. J. *Inorg. Chem.* **1988**, *27*, 4587.
(40) Forster, R. J.; Vos, J. G. *Macromolecules* **1990**, *23*, 4372.
(41) Gaudiello, J. G.; Bradley, P. G.; Norton, K. A.; Woodruff, W. H.; Bard, A. J. *Inorg. Chem.* **1984**, *23*, 3.

acidified with BF_3·OEt_2. In situ conductivity measurements were carried out with polymer-coated interdigitated microelectrode arrays. The results indicate that charge transport rates can be significantly enhanced by matching of redox potentials of metal center and bridge states and by use of conjugated bridges. The maximum absolute DC conductivity of the quaterthienyl-bridged {Ru(tpy)$_2$} and {Os(tpy)$_2$} polymers was determined to $1.6(\pm 0.3) \times 10^{-3}$ S cm^{-1} irrespective of the identity of the metal center.

Acknowledgment. J.H. and A.H. gratefully acknowledge financial support from the Swedish Science Research Council (Grant K 5104-20006267/2000).

IC049221M